

# Repurposing Hydrocarbon Wells for Geothermally-heated Horticulture in the UK

William Nibbs<sup>1\*</sup>, Rob Westaway<sup>†</sup>, Gioia Falcone<sup>1</sup>

<sup>1</sup> James Watt School of Engineering, University of Glasgow, Glasgow, G12 8QQ, UK;

\*w.nibbs.1@research.gla.ac.uk

**Keywords:** UK, deep geothermal, repurposing, closed-loop, direct-use, horticulture.

## ABSTRACT

Despite an abundance of accessible subsurface heat, geothermal energy remains under-exploited in the UK, lagging the progress made by other European countries. By repurposing abandoned hydrocarbon wells, geothermal technologies – for example, deep borehole heat exchangers (DBHEs) – can ‘mine’ low-enthalpy energy from the subsurface while avoiding new drilling costs, thus reducing financial risks. Previous work has determined the most suitable candidates for geothermal repurposing using a systematic data-screening analysis of onshore UK hydrocarbon wells (Watson *et al.*, 2020). The research herein aimed to predict the thermal performance of a single-well candidate site (KM-8), in the Kirby Misperton gas field of North-East England, and assess its feasibility for commercial greenhouse spatial heating. A dual-continuum numerical model is implemented in MATLAB<sup>®</sup> to determine DBHE thermal power outputs, including site-specific geology borehole dimensioning and temperature-dependent material properties. Greenhouse energy modelling is performed using a commercial greenhouse simulation software (Hortinergy<sup>®</sup>) including: local weather forecasting; greenhouse dimensioning, materials and screens; desired internal climate settings; and greenhouse configuration (conventional (open), semi-closed or closed). Greenhouse load-following DBHE operating conditions are met by PID circulation flow-rate control in conjunction with a plate heat-exchanger and heat pump system at surface. The parasitic loads, emissions savings and economic feasibility of the system are also considered. The study shows that repurposing KM-8 has the potential to meet annual heating demands of a commercial-scale greenhouse. Repurposing abandoned wells presents a tangible opportunity to harness the UK geothermal resource as a strategic clean alternative to natural gas in greenhouse horticulture; supplying thermal energy to a ‘green’ greenhouse market post-Brexit. Facilitating knowledge and skills transfer between the petroleum and geothermal sectors will accelerate the decarbonisation of greenhouse heating, improving the sustainability of food production.

## 1. INTRODUCTION

The UK continues to seek scalable low-carbon energy solutions to the challenge of heat decarbonisation. Despite legislating on net-zero for 2050, renewable or sustainable sources account for less than 7% of the UK’s total heat supply which constitutes the most sizeable portion (*c.* 45%) of the UK’s total energy demand; in comparison to transport (*c.* 41%) and electricity (*c.* 14%) (BEIS, 2021a). With recent geopolitical developments, both foreign and domestic, the decarbonisation of heat continues to pose a significant challenge in resolving the energy trilemma (WEC, 2021). Recent estimates of the UK’s geothermal resources suggest that geothermal energy in its various forms could play an important role in addressing this challenge (Gluyas *et al.*, 2018; Abesser and Walker, 2022).

Deep Geothermal Single Wells (DGSWs), defined here as any geothermal scheme extending beyond depths of 500m, and constrained to a single borehole only, offer an alternative to systems reliant on suitable subsurface properties (porosity and permeability) or reservoir stimulation. In DGSWs, geothermally-heated fluid extracted from the borehole is passed through a heat exchanger and/or heat pump at surface before being discharged (open-loop) or reinjected (closed-loop). While there are many variations of such systems, as described in detail in Westaway (2018), the work herein focuses on the closed-loop co-axial Deep Borehole Heat Exchanger (DBHE) configuration (Fig. 1). Composed of concentric piping along the length of the borehole, the DBHE considered herein injects a working fluid into a vertical annulus to draw heat via conduction from the surrounding rock before being rapidly returned to surface via a narrow insulated central production pipe. The mined heat is exchanged at surface and working fluid reinjected to complete the closed-loop cycle. The system is reliant on conduction only from the subsurface surroundings and thus not directly dependent on a comprehensive knowledge of local hydraulic transport properties. Furthermore, the closed-loop nature of the DBHE precludes the extraction of geofluids, further simplifying system operation.

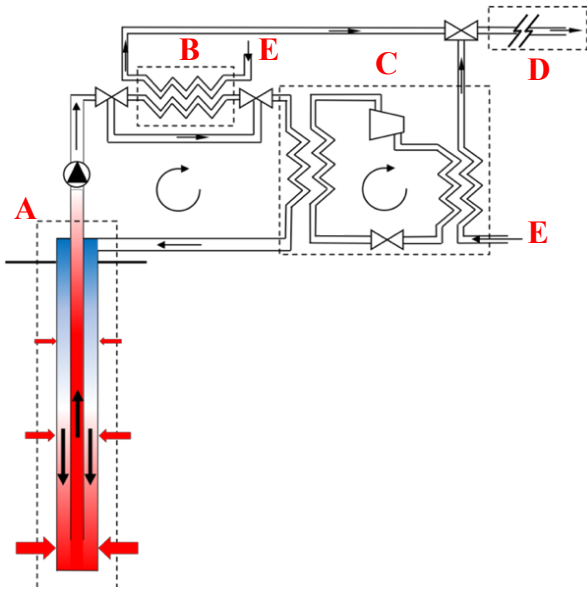


**Figure 1: Schematic of system used to sustain ideal indoor growing conditions of a commercial greenhouse. Power flow pathway as follows: (A) Deep borehole heat exchanger; (B) Plate heat-exchanger; (C) Compression heat-pump; (D) Heat distribution pipe to heat load and (E) Return flow from heat load. Energy system adapted from Westaway (2018).**

Despite minimising the need to substantiate the thermo-chemical-mechanical-hydraulic properties of the local geological strata, deep geothermal energy projects remain inexorably linked with the financial risks of high capital expenditure and technical uncertainty. In the absence of low-cost ultra-deep (*i.e.* >10km) drilling capabilities, the majority of accessible UK geothermal energy exists in the low-enthalpy regime (with the exception of localized geological anomalies). Temperatures of the order of 40°C, 90°C and 140°C are therefore typical at depths of 1km, 3km and 5km, respectively (Abesser *et al.*, 2020). The potential for efficient electricity production is limited at these temperatures, particularly as heat conduction is confined to the contact area between the DBHE and host formations. It is anticipated therefore that such systems will more efficiently facilitate low-enthalpy heat extraction from the subsurface.

The low power density per well in the UK geothermal context exacerbates the financial risks associated with unproven resources. Many have therefore highlighted the potential of repurposing hydrocarbon wells as DGSWs (for example, Davis and Michaelidis, 2009; Nian *et al.*, 2019; Hu *et al.*, 2020). This offers a potentially substantial reduction in capital costs by removing drilling costs that account for ~65% of total capital expenditure (ARUP, 2021), while also reducing subsurface uncertainty using existing wellbore data. Despite the potential benefits of upcycling abandoned hydrocarbon liabilities into decarbonisation assets, current UK regulation prevents the repurposing of

hydrocarbon wells. The work herein thus considers a site-specific pre-feasibility study under the working assumption that future amendments will permit geothermal energy extraction from repurposed wells.

Working under the same assumption on regulation reform, previous work has used a multi-parameter screening survey to highlight the most favourable onshore wells in the UK for geothermal repurposing (Watson *et al.*, 2020). Of the 2242 existing onshore wells (both in production and at end-of-life), Watson *et al.*, (2020) identify 560 high-performing candidates that offer potential as geothermal energy sites (Fig. 2). Further screening for near-vertical wells – improving the applicability of DBHE repurposing – reduces the number of candidates to approximately 73 existing wells. As a case study, the work herein investigates the technical feasibility of repurposing the KM-8 gas well located in the Kirby Misperton gas field of north-east England, and subsequently studies its potential to meet the spatial heat demand of a commercial-scale greenhouse.

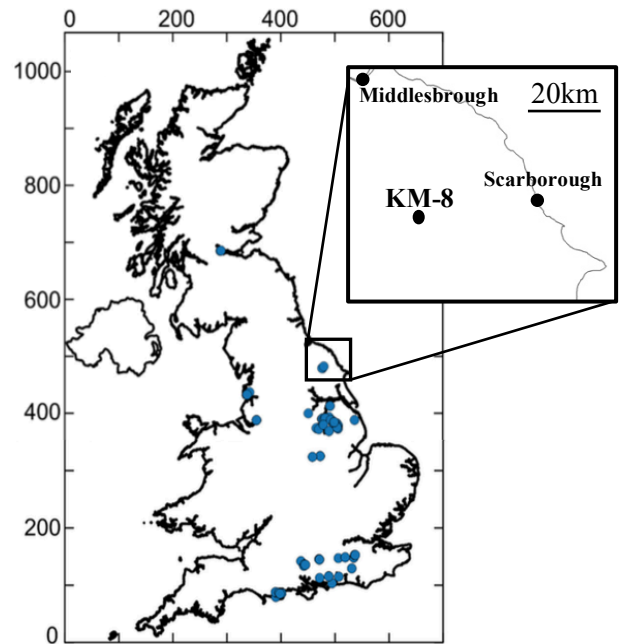


**Figure 2: Candidate onshore hydrocarbon wells for geothermal repurposing (blue dots) at 100km grid resolution (Watson *et al.*, 2020) and, inset, Kirby Misperton well 8 (KM-8) location in NE England.**

## 2. DEEP BOREHOLE HEAT EXCHANGER MODEL

This study uses a dual-continuum model with finite-difference solver, adapted from the numerical model of Brown *et al.* (2021) which applies earlier work (Al-Khoury *et al.*, 2005; Al-Khoury and Bonnier, 2006) to the context of DBHE applications in the Cheshire Basin of north-west England. By adapting this model in MATLAB<sup>®</sup> to include the heterogeneity of site-specific sub-crop stratification and thermal-dependent material properties, the connection between subsurface low-enthalpy geothermal potential and surface direct-heat

applications can be examined. To reduce model computational demands while maintaining geological accuracy, the dual-continuum method represents the DBHE as a one-dimensional (1D) line source/sink and the surrounding geological strata as a three-dimensional (3D) collection of nodes with conductive heat flow defined by the heat equation:

$$\frac{\partial T}{\partial t} = \alpha \nabla^2 T \quad [1]$$

where  $T$  and  $\alpha$  represent the temperature and thermal diffusivity of the surrounding rock, respectively, and  $\partial t$  the time step.

Thermal resistance to conductive heat transfer has previously been shown to act analogous to electrical resistance under steady-state conditions. The initial transient phase experienced at DBHE start up prior to quasi-steady-state conditions, renders this analogy with electrical resistances an approximation of thermal resistance herein, and includes the additional assumption of 2D radial heat flow (Brown *et al.*, 2021). Furthermore, the lateral temperature variation within the casings of the concentric DBHE structure is not modelled; assuming the variation within each of the thin layers to be negligible. The heat flux in annulus and production pipes of the DBHE, as well as the cement and surrounding rock, are modelled at each time step and node using the partial differential equations:

$$\rho_f c_f \frac{\partial T_p}{\partial t} A_p - \lambda_f \frac{\partial^2 T_p}{\partial z^2} A_p - \rho_f c_f u_p \frac{\partial T_p}{\partial z} A_p = b_{pa} (T_a - T_p) 2\pi r_{po} \quad [2]$$

$$\rho_f c_f \frac{\partial T_a}{\partial t} A_a - \lambda_f \frac{\partial^2 T_a}{\partial z^2} A_a + \rho_f c_f u_a \frac{\partial T_a}{\partial z} A_a = b_{pa} (T_p - T_a) 2\pi r_{po} + b_{ac} (T_c - T_a) 2\pi r_{ai} \quad [3]$$

$$\rho_c c_c \frac{\partial T_c}{\partial t} A_c - \lambda_c \frac{\partial^2 T_c}{\partial z^2} A_c = b_{ac} (T_a - T_c) 2\pi r_{ai} + b_{cr} (T_r - T_c) 2\pi r_{co} \quad [4]$$

$$\rho_r c_r \frac{\partial T_r}{\partial t} A_r - \lambda_r \frac{\partial^2 T_r}{\partial z^2} A_r = b_{cr} (T_c - T_r) 2\pi r_{co} \quad [5]$$

where  $T$  represents the temperature in a given medium (all subscripts defined in Fig. 3). The properties  $\rho$ ,  $c$  and  $\lambda$  are density, specific heat capacity and thermal conductivity of the concentric DBHE materials, respectively, and modelled to vary with down-hole temperatures. The heat transfer coefficients ( $b$ ), the reciprocal of the thermal resistances (shown in Fig. 3) are modelled between the concentric media and include the convective heat transfer coefficient when the circulating fluid is in motion at a velocity ( $u$ ). The variables  $A$  and  $r$ , represent the physical properties of axial cross-sectional areas and pipe radii, respectively (subscripts defined in Fig. 3).

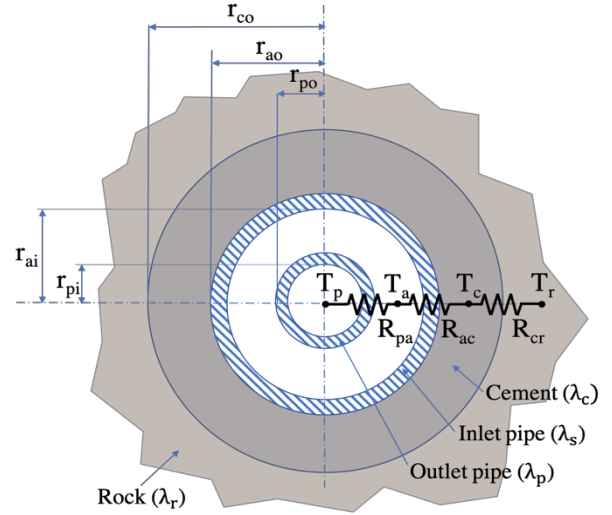


**Figure 3: Cross-section of co-axial deep borehole heat exchanger (not to scale). Subscript indexing of temperatures ( $T$ ), thermal resistances ( $R$ ) and thermal conductivities ( $\lambda$ ): p = production pipe, a = injection annulus, c = cement, r = rock, s=outer steel casing, pa = production pipe-annulus interface, ac = annulus-cement interface, cr = cement-rock interface. Radii subscript indexing: i = inner surface, o = outer surface, and preceding indices a, c, and p follow from above.**

The model uses a finite-difference approach to solve the spatial and temporal partial differential equations of the 1D and 3D domains for each time step. The first-order derivatives are solved by forward and backward difference approximations due to the unstable nature of the central difference technique while the second order derivatives are solved in MATLAB<sup>®</sup> using the discrete finite-difference approximation to the Laplacian differential operator. The orthogonal 3D mesh applied to the thermally active rock is solved explicitly for a mesh of radially-increasing node-spacing – with an inner-most lateral mesh spacing of 0.4m increasing exponentially to the mesh boundary set as the radius of thermal influence (defined as  $2\sqrt{at}$  where  $t$  is the total time of DBHE fluid in circulation). The 1D borehole is solved implicitly due to the discrepancies in computational intensity between explicit and implicit solvers – implicit solving being more demanding – and the large number of nodes in the 3D mesh in comparison with the 1D line model (Brown *et al.*, 2021). Both nodal representations have a vertical spacing ( $\partial z$ ) of 20m. Solving the heat transfer equations allows the output temperature of the DBHE ( $T_{out}$ ) to be calculated, and with knowledge of the injection temperature ( $T_{inj}$ ), specific heat capacity of the circulating fluid ( $c_f$ ) and the mass flow rate ( $\dot{m}_f$ ), the thermal power output ( $\dot{Q}_{DBHE}$ ) at each time step is calculated using:

$$\dot{Q}_{DBHE} = \dot{m}_f c_f (T_{out} - T_{inj}) \quad [6]$$

### 3. CASE STUDY: REPURPOSING THE KM-8 GAS WELL

Westaway (2018) emphasised the need to include site-specific variables into any DBHE model and divided them among two distinct categories of importance: (i) subsurface geological properties (for example, geothermal gradient predictions and multi-layer formations representation) and (ii) accurate predictions of end-user demand profiles used in dictating operational parameters of DBHE control. These two areas are addressed for the KM-8 gas well of north-east England to assess DBHE performance as a sustainable heat supply.

#### 3.1 KM-8 Well Background

The Vale of Pickering, North Yorkshire (UK) has been the focus of considerable onshore natural gas extraction – targeting conventional Permian reservoirs and proposed hydraulic fracturing of the Carboniferous Bowland sequence of the Cleveland Basin (an onshore extension of the Southern North Sea gas basin). Located within the vale, the Kirby Misperton gas field (split across well pads KMA and KMB) contains several abandoned exploration and production wells. The vertical KM-8 exploration well is one such example aimed at onshore shale gas extraction. Drilled by Third Energy in 2013, the well reaches 3099m (10167ft) true vertical depth (TVD) – 3112m (10210ft) measured depth (MD) – and was intended to replicate the nearby KM-1 gas well. Drilling failed to reach the target Namurian sandstone at 3621m (11880ft) MD due to borehole stability (Hughes *et al.*, 2018). Despite failing to reach the intended bottom-hole depth, hydraulic fracturing proposals were granted for shale gas extraction at shallower intervals of the Namurian Bowland Shale. The approval to proceed with extraction faced considerable public and community backlash and consequently the decision was made to abort hydrocarbon production at the site. As the area coincides with above-average surface heat flow estimates, repurposing this hydrocarbon well to extract low-enthalpy geothermal energy from the subsurface may offer a low-carbon alternative to hydrocarbon extraction (Busby, 2014; Watson *et al.*, 2020).

#### 3.2 Numerical Model Parameterisation

The sensitivity of DBHE thermal power outputs to engineering and geological parameterisation has been demonstrated through many prior studies (for example, Chen *et al.*, 2019; Hu *et al.*, 2019; Liu *et al.*, 2019). These include sensitivity to circulating flow rates, (re)injection temperatures, casing dimensioning, material thermal conductivity assumptions, and thermal gradients, among others. The material properties and borehole dimensioning used in this study are shown in Table 1, and the sensitivity of the modelling approach used herein to such variables is described in Brown *et al.* (2021) for the case of the Cheshire Basin.

**Table 1: Parameters of deep borehole heat exchanger used in the KM-8 gas well, where ‘Var’ indicates variable parameter values due to temperature dependency or site-specific conditions.**

Parameter (unit)	Value
Depth (m)	3099
Borehole diameter (m)	0.216
Annulus actual diameter (m)	0.159
Inner production pipe actual diameter (m)	0.057
Thickness of outer pipe casing (m)	0.010
Thickness of inner pipe casing (m)	0.008
Thickness of cement (m)	Var
Surface roughness (annulus) ( $10^{-3}$ m)	0.05
Surface roughness (inner pipe) ( $10^{-3}$ m)	0.005
Thermal conductivity (outer pipe) (W/mK)	Var
Thermal conductivity (inner pipe) (W/mK)	Var
Density of rock ( $\text{kg/m}^3$ )	Var
Thermal conductivity of rock (W/mK)	Var
Thermal diffusivity of rock ( $\text{m}^2/\text{s}$ )	Var
Specific heat capacity of rock (J/kgK)	Var
Density of cement ( $\text{kg/m}^3$ )	1500
Thermal conductivity of cement (W/mK)	Var
Specific heat capacity of cement (J/kgK)	Var
Density of fluid ( $\text{kg/m}^3$ )	1000
Thermal conductivity of fluid (W/mK)	Var
Specific heat capacity of fluid (J/kgK)	Var
Surface temperature ( $^{\circ}\text{C}$ )	10
Fluid injection temperature ( $^{\circ}\text{C}$ )	10
Thermal gradient ( $^{\circ}\text{C}/\text{km}$ )	32
Initial bottom hole temperature ( $^{\circ}\text{C}$ )	107

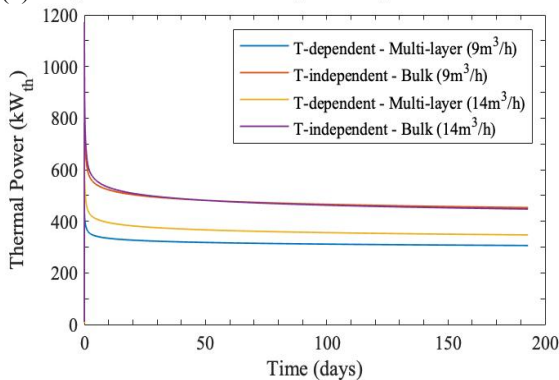
In the case of well repurposing there is limited scope to significantly alter well diameters, particularly when non-bespoke, standard pipe dimensions are considered. The sensitivity analysis thus considers fixed pipe diameters and thicknesses for the steel casing and cement. However, as a result of the borehole spudding process the thickness of the encasing cement varies along the depth of the well. This variation in thickness will impact the feasible heat transfer to the inner fluid and has therefore been incorporated into the numerical model to improve the site-specific representation of KM-8 as a DBHE. At depths below 1882m (6175ft) the borehole diameter is 0.216m (8.5 inches). This is larger than dimensions in similar studies (*c.* 0.178m (7-inch)) which will allow lower flow velocities in the annulus for the same mass flow rates, thus increasing heat gain into the fluid due to greater residency times.

Modelling DBHEs in repurposed wells benefits from publicly-available well tops data, describing the depth and thickness of each formation encountered along the length of the borehole (UKOGL, 2021). The KM-8 well encountered 24 formations, which vary greatly in thickness and composition – producing varying thermal conductivity and diffusivity values. Insights into the formation of the Vale of Pickering have benefitted from extensive documentation of the Quaternary (BGS, 2015), but at present few data are available for strata overlain by the Kimmeridge Clay Formation, Corallian



Group and Oxford Clay Formation. The Carboniferous Bowland Shale reservoir at depths of 2-3km is overlain by a complex series of Jurassic, Triassic and Permian sedimentary rocks, and the thickness of the Carboniferous Bowland sequence – a mudstone group with 25-65% quartz content – creates considerable heterogeneity in thermo-physical properties. As seen from equations [2-5], these thermo-physical values determine the heat extracted from the surrounding rock over time and are therefore important when considering the long-term thermal power output of the DBHE. Where analytical models may offer adequate representations of shallow BHE designs, these approaches reduce in validity as the depth of the BHE increases and the implications of multi-layer stratification become a more significant source of systematic error in the model. Given the formation type, thermal properties have been estimated and incorporated into the numerical modelling herein, creating a multi-layer approach which is shown to impact the rate of decline in thermal power and eventual pseudo steady-state thermal power output when compared to bulk approximations typically used in DBHE modelling (Fig. 4). Using the simplifying assumption of constant formation thickness propagating radially from the DBHE allows more localised estimates of thermal diffusivity values to be used in each formation of the subsurface strata.

(a) Comparison of DBHE thermal power output at constant flow rates



(b) Comparison of DBHE output temperature at constant flow rates

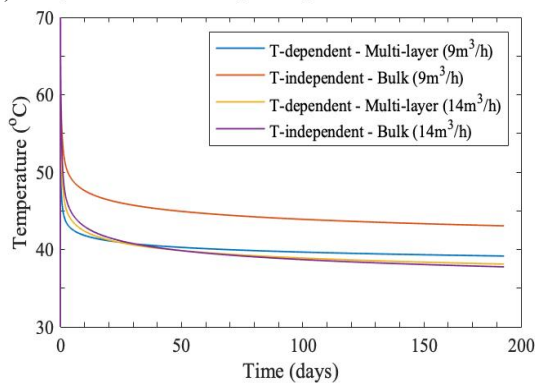


**Figure 4: The impact of subsurface stratification approximations and temperature(T)-dependent material properties on the numerical modelling of (a) DBHE thermal power outputs and (b) DBHE flow temperature outputs.**

The thermal gradient for the Cleveland Basin (predicted to be 32°C/km) has been derived from heat flow measurements in relatively shallow wells (Downing and Gray, 1986; Busby, 2014) which has been demonstrated to incur extrapolation errors by ignoring local paleoclimate corrections arising from the near-surface chilling effects of historic glaciation events (Westaway and Younger, 2013). Applying the method defined by Westaway and Younger (2013) produced an estimated 9 mWm<sup>-2</sup> corrective increase in heat flow – corresponding to a corrected geothermal gradient of 35.6°C/km. This created a 7.6% difference in the quasi-steady-state thermal power output of the DBHE after three months of continuous operation at 11m<sup>3</sup>/h. Topographic corrections have not been applied.

### 3.3 Direct-Use of Low-Enthalpy Closed-Loop System

DBHE output temperatures and flow rates must be managed to produce value to an end user, of which there are potentially many (Lindal, 1973). The area surrounding the Kirby Misperton well pads is sparsely populated and consists of largely agricultural land. The area may therefore make a promising location for food production in commercial-scale greenhouses.

Commercial greenhouses are, per hectare, an energy intensive method of food production; dependent on geography, crop species, greenhouse control systems and energy source (typically natural gas) (Coomans *et al.*, 2013). Geothermal energy as a low-carbon spatial heating alternative to natural gas in commercial food-producing greenhouses has yet to be deployed in the UK but has been demonstrated in a number of projects in continental Europe. Recent efforts to decarbonise the UK food supply has seen the development of two large glasshouses in Norwich and Bury St. Edmunds in south-east England. The £120M project, aims to heat greenhouses via a cascading heat pump scheme using waste heat from waste water facilities as a primary energy source (Lattimore, 2019). The physics-based modelling of the DBHE in the repurposed KM-8 well is extended to the greenhouse end-use case to assess the sustainable spatial heating potential of a closed-loop geothermal system in the UK.

The commercial greenhouse modelling software Hortinergy<sup>®</sup> has been used to create an accurate forecast of diurnal and seasonal fluctuations in heat load. The software allows the grower to tailor the greenhouse design and configuration to meet the needs of the crops and uses location-specific weather predictions to anticipate the heat requirements for sustained optimal indoor growing conditions (Hortinergy, 2022). The model also reflects the impact that regulation of indoor humidity and carbon dioxide concentrations has on the hourly thermal power demands throughout the year. In this case study, a contemporary semi-closed glasshouse has been selected to support tomato production – given the crop's popularity in the UK (*c.* 167 tonnes per day (Lattimore, 2019)). The semi-closed configuration relies on an air-treatment corridor, responsible for

monitoring and optimising the properties of the inputted air before delivery to the body of the greenhouse via perforated tubing parallel to crop beds (Fig. 5) (Sapounas *et al.*, 2020).

The greenhouse model sets lower indoor temperature limits at 20°C and 18°C for day and night cycles, respectively, and a constant upper indoor temperature limit at 25°C (Van Ploeg and Huevelink, 2005). The regulation of relative humidity of the circulating air flow assumes a lower limit on relative humidity at 60%,

however a 90% maximum relative humidity is applied during the day while a 95% night-time relative humidity is applied.

The DBHE extraction flow rate is regulated via Proportional-Integral-Derivative (PID) control to meet the indoor growing conditions. This relies on the closed-loop feedback of errors arising from the differences between DBHE output powers and end-user heating set points. The PID gains were tuned via inspection of the DBHE model sensitivity.

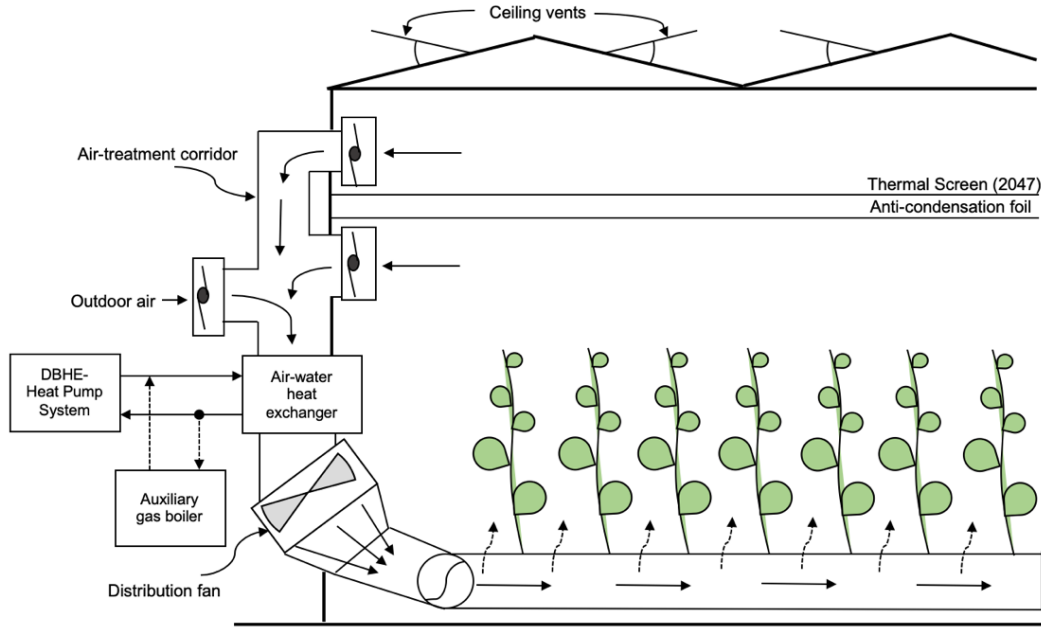


**Figure 5: Semi-closed greenhouse configuration adapted from the Sint-Ksteljine-Waver design described in Coomans *et al.* (2013).**

The pumping power demand for a given flow rate is derived from an understanding of the pressure loss, or pump head, due to friction in the system, calculated using the Darcy-Weisbach relation:

$$\Delta P = \frac{f_D \rho V^2}{4r_i} \quad [7]$$

where  $f_D$  is the Darcy friction factor given by the Tsal approximation of the Colebrook’s equation dependent on the surface roughness estimates for the inner and outer pipes. Thus, the work of the DBHE circulation pump ( $W_{CP}$ ), assuming inlet and outlet pressures are constant and equal, is calculated using:

$$W_{CP} = \frac{\Delta P \cdot \dot{m}_f}{\rho_f \eta} \quad [8]$$

where  $\dot{m}_f$  is the mass flow rate of the circulating fluid in kg/s,  $\rho_f$  is the fluid density, and  $\eta$  is the pump efficiency (assumed to be 50%). Applying equations [7-8] showed that the thermosiphon effect (due to the buoyancy of temperature-induced density variations in the heated circulating fluid) reduced circulation pumping power in the order of 1% at the highest flow rates (*c.* 14m<sup>3</sup>/h) and is thus ignored in the remaining analysis. This result is in agreement with similar studies

(*c.* 1.8% (Chen *et al.*, 2019)), suggesting that the thermosiphon effect is negligible at the depths and geothermal gradient considered herein while using water as the circulating fluid.

The thermal power of the DBHE output is coupled with a heat exchanger and heat pump at surface to tailor the power delivered to the greenhouse. Adding a heat pump brings the DGSW fluid reinjection temperature in line with ambient surface temperature to maximise DBHE performance (Westaway, 2018). The mean Coefficient of Performance ( $COP_{Mhp}$ ) of the heat pump is derived from Baster (2011) and given by:

$$COP_{Mhp} = \frac{1}{T_I - T_S} \int_{T_S}^{T_I} COP_{hp} dT \quad [9]$$

where  $T_I$  and  $T_S$  are the DBHE output and ambient surface temperatures, respectively, and the instantaneous COP of the heat pump ( $COP_{hp}$ ) is assumed to vary as:

$$COP_{hp} = 6.70 \exp(-0.022 \cdot (T_G - T)) \quad [10]$$

where  $T_G$  represents the demand temperature from the greenhouse. For a single heat pump at surface, the

thermal power delivered to the greenhouse is next calculated using:

$$\dot{Q}_G = \frac{COP_{Mhp}}{COP_{Mhp} - 1} \cdot \dot{Q}_{DBHE} \quad [11]$$

where  $\dot{Q}_{DBHE}$  is the thermal power out of the DBHE at each time step of the model. The mean work required for the single heat pump at surface is therefore given by:

$$W_{Mhp} = \frac{\dot{Q}_G}{COP_{Mhp}} = \frac{1}{COP_{Mhp} - 1} \cdot \dot{Q}_{DBHE} \quad [12]$$

and the Coefficient of System Performance (CSP) (including the pumping power requirements) can be calculated at each time step for a single stage heat pump

using:

$$CSP = \frac{\dot{Q}_G}{W_{Mhp} + W_{CP}} \quad [13]$$

where WCP is the required work of the circulation pump. The ability of the DBHE to meet the greenhouse heat loads over an annual growing period can henceforth be assessed by combining the subsurface numerical modelling with the surface calculations of work, demand and final thermal power delivery (Fig.6). For the greenhouse and DBHE system modelled, an average annual CSP of 4.64 was calculated, highlighting the efficiency of the system in meeting the demand. Over the course of the growing period a Mean Average Percentage Error (MAPE) of 1.27% was recorded.

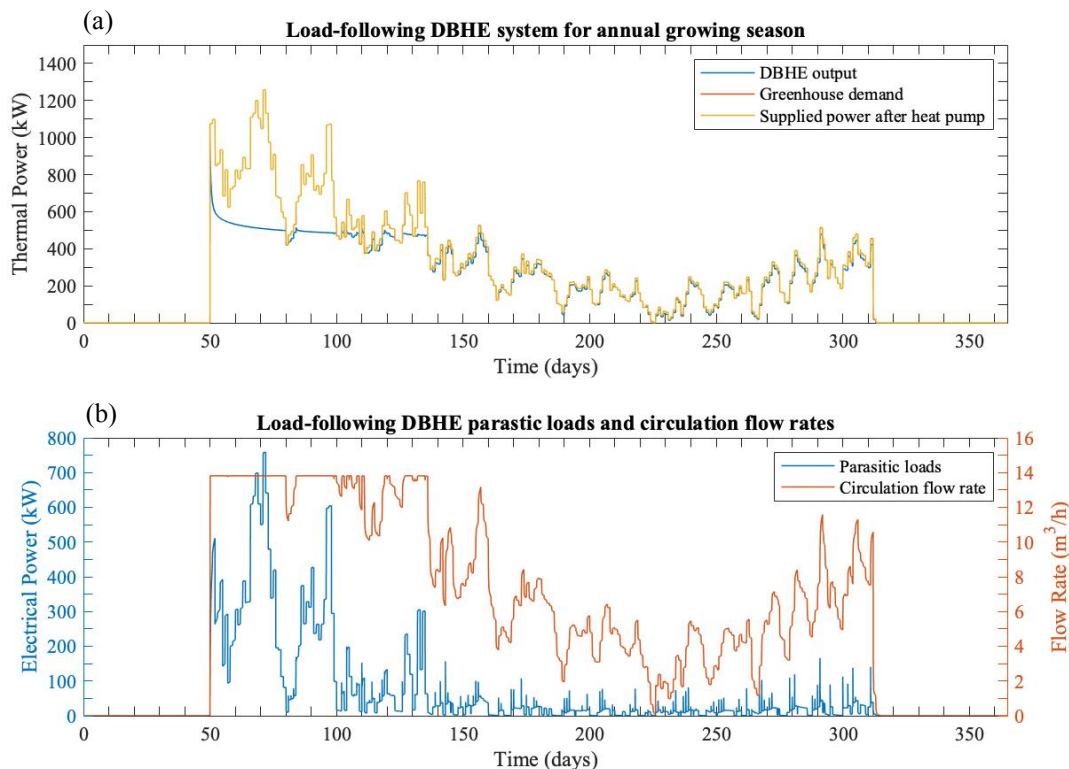


**Figure 6: Demand-following response of the DBHE at daily resolution over the growing season for a 10000m<sup>2</sup> semi-closed commercial greenhouse. (a) The greenhouse demand compared with heat pump and DBHE outputs. Errors between the greenhouse demand and the thermal power supplied are small and thus indistinguishable at the resolution plotting. (b) The total power consumed by the heat pump compressor and circulation pump in meeting greenhouse demand and maintaining flow rates.**

The Net-Present Value (NPV) metric has been used to provide a preliminary assessment of the financial viability of KM-8 well repurposing, using.

$$NPV = \left[ \sum_{t=0}^N \frac{R_t}{(1+i)^n} \right] - IC \quad [14]$$

where  $i$  and  $n$  are the interest rate and cashflow time, respectively (assumed here on an annual basis). The net annual cashflow ( $R_t$ ) is derived from the difference in annual revenues from heat sales and annual operational costs. The operational costs can be estimated by

summing the total work requirements for the heat pump and circulation pump over the year. The electricity cost was set at £0.1308/kWh – an approximate retail price for a large industrial consumer (BEIS, 2021b). The expected revenues are the product of total heat delivered and the price of heat; a subsidy-free price is set at £0.0300/kWh – as used in GEL (2016) and Westaway (2018). A comparison in NPV is drawn between this subsidy-free example and a case including a subsidy – similar to the Renewable Heat Incentive (RHI) – which is set at an additional heat price of £0.0503/kWh (OFGEM, 2021). The initial cost (IC), or capital expenditure, has been estimated from recent



financial analysis of a DGSW project in the UK (GEL, 2016). Removing the need for drilling significantly reduces the IC, estimated here as £1.08M (including a 10% contingency). This shows substantial reductions from the £2.29M proposed spend for the AECC project – a DGSW of similar scale which would require £1.35M for drilling alone (GEL, 2016). The annual NPV over a 20-year period is shown in Fig. 7. This shows the cases of DBHE at a constant flow rate (14m<sup>3</sup>/h) and the demand-following flow-rates used when supplying the commercial-scale greenhouse modelled above. From initial modelling, the economic case for the KM-8 DBHE appears marginal in the absence of a RHI-style subsidy although this is highly dependent on the operating conditions of the DBHE.

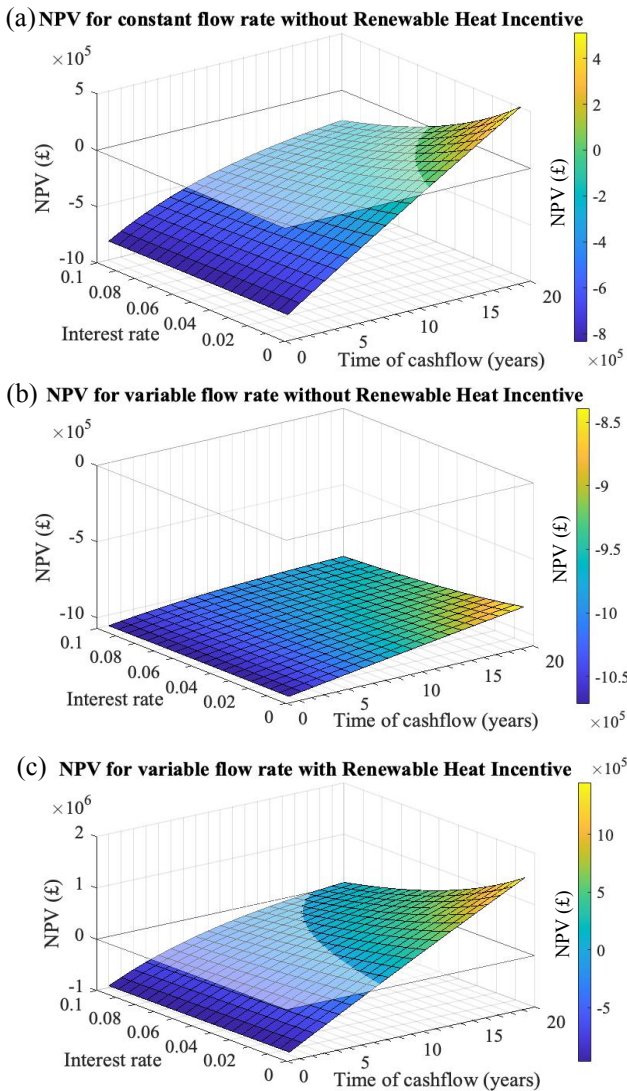


**Figure 7: Net-Present-Value (NPV) analysis of the DBHE performance over a 20-year period, when revenue incomes are (a) Without a RHI-style subsidy at a constant flow rate of 14m<sup>3</sup>/h, (b) Without a RHI-style subsidy at demand-following flow rates and (c) With a RHI-style subsidy at demand-following flow rates. The horizontal plane represents £0 NPV to visualise the predicted cross-over.**

#### 4. CONCLUSIONS

The work herein extends previous work on repurposing hydrocarbon wells to consider variable end-user demand profiles while including site-specific well-log data and temperature-dependent material properties. The simulations provided in this work suggest that at a constant flow rate of 14m<sup>3</sup>/h the DBHE is capable of providing over 370kW<sub>th</sub> at pseudo-steady-state after six months of operation, though declining gradually with further heat extraction. When used in direct connection with variable loads such as the commercial-greenhouse modelled herein, the temporal variation in flow rates enables thermal recovery of the DBHE, extending the lifetime of the system yet potentially weakening the economic incentive for the project.

The high-level economic analysis carried out indicates the importance of subsidies when repurposing a hydrocarbon well for low-carbon spatial heating of a commercial greenhouse (Fig. 7). This result is however subject to a number of localised approximations and conditions, as well as system design decisions. For example, improved heat conduction could be achieved by altering DBHE material properties, including highly conductive graphite for example. Furthermore, existing borehole conditions need to be considered including borehole stability issues and practical pipe installation concerns such as the presence of existing down-hole cement. Finally, the greenhouse modelling software does not account for changes in greenhouse heating demand beyond a single year. The economic case therefore assumes equal greenhouse demand and DBHE supply capabilities for the 20-year period. Although acting as an initial high-level analysis, the modelling does not capture the change in greenhouse demand or DBHE thermal drawdown beyond the first year of operation.

Future work should aim to provide a more detailed study into the economic case for onshore hydrocarbon well repurposing in the UK. This work should consider the potential of DBHEs as part of multi-vector district heating and cooling networks, as well as the cases of larger commercial greenhouses and annual variations in greenhouse demand profiles. Continuous operation of the DBHE or use as a means of thermal energy storage in other applications are likely to improve the business case for the repurposed well. The mode of DBHE operation has clear implications for the financial viability of the system and should be optimised to maximise the benefits that well repurposing can offer in the energy transition.

#### REFERENCES

Abesser, C. and Walker, A., Geothermal Energy. *UK Parliament POST*. Retrieved from: <https://post.parliament.uk/research-briefings/post-pb-0046/> (2022).

Abesser, C. B. J. P., Pharoah, T. C., Bloodworth, A. J and Ward, R. S. Unlocking the potential of geothermal energy in the UK, *British Geological*



- Survey Open Report*, vol. OR/20/049, (2020) pp. 1-22.
- Al-Khoury, R., and P. G. Bonnier. Efficient finite element formulation for geothermal heating systems. Part II: transient. *International journal for numerical methods in engineering* 67, no. 5 (2006): 725-745.
- Al-Khoury, R., Bonnier, P. G., and Brinkgreve, R. B. J. Efficient finite element formulation for geothermal heating systems. Part I: Steady state. *International journal for numerical methods in engineering* 63, no. 7 (2005): 988-1013.
- Alimonti, C. and Soldo, E., "Study of geothermal power generation from a very deep oil well with a wellbore heat exchanger.," *Renewable Energy*, vol. 86., (2016) pp. 292-301,
- ARUP, Deep Geothermal Energy: Economic Decarbonisation Opportunities for the United Kingdom (2021) Retrieved from: Deep-Geothermal-Energy-Opportunities-for-the-UK.pdf.
- Baster, M. "Modelling the performance of air source heat pump systems," MSc thesis, Strathclyde University <[http://www.esru.strath.ac.uk/Documents/MSc\\_2011/Baster.pdf](http://www.esru.strath.ac.uk/Documents/MSc_2011/Baster.pdf)>, Glasgow, (2011).
- BEISa, "Digest of UK Energy Statistics Annual data for UK, 2020," (2021a). [Online]. Available: [https://assets.publishing.service.gov.uk/government/uploads/system/uploads/attachment\\_data/file/1007132/DUKES\\_2021\\_Chapters\\_1\\_to\\_7.pdf](https://assets.publishing.service.gov.uk/government/uploads/system/uploads/attachment_data/file/1007132/DUKES_2021_Chapters_1_to_7.pdf). [Accessed 4 Aug 2021].
- BEISb, "Quarterly Energy Prices UK: January to March 2021," (2021b). [Online]. Available: [https://assets.publishing.service.gov.uk/government/uploads/system/uploads/attachment\\_data/file/997483/Quarterly\\_Energy\\_Prices\\_June\\_2021.pdf](https://assets.publishing.service.gov.uk/government/uploads/system/uploads/attachment_data/file/997483/Quarterly_Energy_Prices_June_2021.pdf). [Accessed 20 July 2021].
- Brown, C. S., Cassidy, N. J., Egan, S. S., & Griffiths, D. Numerical modelling of deep coaxial borehole heat exchangers in the Cheshire Basin, UK. *Computers & Geosciences*, 152, (2021) 104752.
- Busby, J. Geothermal energy in sedimentary basins in the UK. *Hydrogeology journal* 22, no. 1 (2014): 129-141.
- Chen, C., Shao, H., Naumov, D., Kong, Y., Tu, K., & Kolditz, O. (2019). Numerical investigation on the performance, sustainability, and efficiency of the deep borehole heat exchanger system for building heating. *Geothermal Energy*, 7(1), (2019) 1-26.
- Coomans, M., Allaerts, K., Wittemans, L., & Pinxteren, D. Monitoring and energetic performance of two similar semi-closed greenhouse ventilation systems. *Energy Conversion and Management*, 76,(2013) 128-136.
- Davis, A. and Michaelidis, E. Geothermal Power Production from abandoned oil wells. *Energy* vol.34, (2009), 866-872.
- Downing, R. A., and D. A. Gray. "Geothermal resources of the United Kingdom." *Journal of the Geological Society* 143, no. 3 (1986): 499-507.
- GEL Ltd., Aberdeen Exhibition and Conference Centre: Feasibility Report for the Low Carbon Infrastructure Transition Programme (LCITP), GEL Ltd. , Aberdeen, (2016)
- Gluyas, J. G., C. A. Adams, J. P. Busby, J. Craig, C. Hirst, D. A. C. Manning, A. McCay et al. Keeping warm: a review of deep geothermal potential of the UK. *Proceedings of the Institution of Mechanical Engineers, Part A: Journal of Power and Energy* 232, no. 1 (2018): 115-126.
- Hortinergy, (2022) Available: <https://www.hortinergy.com/> [Accessed 29 June 2021].
- Hu, X., Banks, J., Wu, L., & Liu, W. V. Numerical modeling of a coaxial borehole heat exchanger to exploit geothermal energy from abandoned petroleum wells in Hinton, Alberta. *Renewable Energy*, 148, (2020) 1110-1123.
- Hughes, F., Harrison, D., Haarhoff, M., Howlett, P., Pearson, A., Ware, D., ... & Mortimer, A. The unconventional Carboniferous reservoirs of the Greater Kirby Misperton gas field and their potential: North Yorkshire's sleeping giant. In *Geological Society, London, Petroleum Geology Conference series* Vol. 8, No. 1, (2018). pp. 611-625). Geological Society of London.
- Lattimore, P. Growing interest: using wastewater to heat Britain's giant greenhouses. *Chartered Institution of Building Services Engineers, The Greenhouse Effect* (2019).
- Lindal, B.,. Industrial and other application of geothermal energy. Armstead H.C.H., ed., Geothermal Energy, UNESCO, Paris, (1973) pp. 135-148
- Nian, Y., Cheng, W., Yang, X., and Xie, K. Simulation of a novel deep ground source heat pump system using abandoned oil wells with coaxial BHE. *International Journal of Heat and Mass Transfer*, vol. 137 (2019), 400-412.

- OFGEM, "Non-Domestic RHI tariff table," 2021. [Online]. Retrieved from: <https://www.ofgem.gov.uk/publications/non-domestic-rhi-tariff-table>. [Accessed 10 July 2021].
- Sapounas, A., Katsoulas, N., Slager, B., Bezemer, R., & Lelieveld, C.. Design, Control, and Performance Aspects of Semi-Closed Greenhouses. *Agronomy*, 10(11), (2020) 1739.
- UKOGL, UK Onshore Geophysical Library - Well: KIRBY MISPERTON 8, (2021). [Online]. Retrieved from: [https://ukogl.org.uk/map/php/well\\_tops.php?wellId=3015](https://ukogl.org.uk/map/php/well_tops.php?wellId=3015). [Accessed 29 July 2021]
- Van Ploeg D. and Heuvelink E., Influence of sub-optimal temperature on tomato growth and yield: a review., *The Journal of Horticultural Science and Biotechnology*, vol. 80, no. 6, (2005) pp. 652-659,.
- Watson, S. M., Falcone, G., and Westaway, R. Repurposing hydrocarbon wells for geothermal use in the UK: The onshore fields with the greatest potential. *Energies* 13, no. 14 (2020): 3541. Westaway, R. Deep geothermal single well heat production: critical appraisal under UK conditions. *Quarterly Journal of Engineering Geology and Hydrogeology* 51, no. 4 (2018): 424-449.
- Westaway, R., & Younger, P. L. Accounting for palaeoclimate and topography: a rigorous approach to correction of the British geothermal dataset. *Geothermics*, 48, (2013). 31-51.
- World Energy Council. World Energy Trilemma Index. World Energy Council. Retrieved from: [http://worldenergy.org/assets/downloads/WE\\_Trilemma\\_Index\\_2021.pdf?v=1649317554](http://worldenergy.org/assets/downloads/WE_Trilemma_Index_2021.pdf?v=1649317554) (2021).

### Acknowledgements

The authors would like to acknowledge Christopher S. Brown from the University of Glasgow for providing access to the initial MATLAB<sup>®</sup> code from which the model presented herein has been derived.